Effect of Static Load Models on Hopf Bifurcation Point and Critical Modes of Power Systems

N. Mithulananthan
Electric Power System Management, Energy Program, Asian Institute
of Technology, P.O. Box 4, Klong Luang, Pathum Thani 12120,
Thailand, e-mail: mithulan@ait.ac.th

C. A. Cañizares
Dept. of Electrical and Computer Engineering, University of Waterloo,
200 University Avenue West, Waterloo, Ontario,
Canada N2 L3G1

Abstract
This paper presents the effect of different static load models on Hopf bifurcation point and critical eigenvalues of power systems. Three most commonly used static load models are investigated thoroughly under various operating conditions and with different power system controllers. Some interesting new observations hase emerged in the damping ratio of the critical mode, especially when power system controllers are introduced for control, in the system to control Hopf bifurcations. These observations would be useful in controller design for Hopf bifurcation or oscillation control.

1. Introduction

Power system oscillations, especially Low-frequency electromechanical oscillations have been a major concern in power system planning and operation as they limit power transfer in the transmission lines and induce stress on various components in power systems. Given the characteristics and nature of these oscillations, these problems can be studied using Hopf bifurcation (HB) theory, which can be used to understand the onset and control of an oscillatory instability problem in power systems [1].

Oscillation problems with its associated HB may arise due to a variety of reasons, namely, variable net damping, frequency dependence of electrical torque and voltage control issues [2], [3] (e.g. fast acting exciters) and are typically triggered by contingencies. The fundamental reason for these types of problems is lack of damping on the critical modes, in most cases, they appear on stressed systems, i.e. heavily loaded systems. This is of particular concern nowadays as many current power networks operate near their stability limits due to economical and environmental constraints.

Some incidents of partial or full power interruptions induced by oscillatory problems and its associated HB, are reported in [4] and [5].

Oscillation problems in power systems can be controlled using a number of controllers. Traditionally, a power system stabilizer (PSS) is employed in the generation side to control this problem [6]. More recently, Flexible AC Transmission System (FACTS) controllers, such as SVC, TCSC, STATCOM, SSSC and UPFC have been utilized and/or shown to be very effective for oscillation control when proper controls and placing techniques are used [1]. HB control through generation re-dispatch and secondary voltage control as well as load shedding techniques have also been proposed as a mechanism for oscillation or HB control in power systems [7], [8].

The challenge in all these control designs is getting more reliable simulation results; hence, proper modeling of various network components is important. In particular, the load characteristics have been shown to have a significant impact on voltage stability, transient

stability and small signal stability studies [9], [10], [11]. Decisions concerning the reinforcement, such as the type and placement of controllers are based on the results of these studies, with load modeling leading to different conclusions. Loads are typically modeled in these studies as constant impedance, constant current and constant power and/or a combination of these models [12]. For example, studies on the Western Electric Coordinating Council (WECC) system in USA, have indicated that using a constant impedance load model with small signal stability tends to overestimate the damping by about 25% when compared to more "accurate" load models [13]. Thus in this paper, an effort is made to better understand the effect of using these typical static load models on the Hopf bifurcation point and damping ratio of the critical modes under various operating conditions, and in the presence of various oscillation control devices.

The rest of this paper is organized as follows: Section 2 explains the basic theory behind HB from the point of view of oscillations. Typical static load models for power system studies are briefly discussed in Section 3, together with the description of the test system and analytical tools utilized for the studies presented here. In Section 4, various simulation results are presented, along with a detailed discussion of various interesting results regarding the effect of load models on the oscillatory behavior of the test system. The main contributions and conclusions of the paper are summarized in Section 5.

2. Hopf Bifurcations

Power system oscillation problems are classically associated with a pair of complex eigenvalues, typically referred to as the "critical eigenvalues," of system equilibrium (operating points). At the point of oscillation, the critical eigenvalue crosses the imaginary axis of the complex plane, from the left half-plane to the right half-plane when the system undergoes sudden changes (e.g. line outages [12]). If the particular oscillatory problem is studied using more gradual changes in the system, such as changes on slow varying parameters like system loading, this issue can be viewed as a HB problem [1], [2], [14].

Periodic orbits or limit cycles that emerge around the equilibrium point characterize HB.

These types of bifurcation are also known as oscillatory bifurcations. In order to explain the basic theory behind HB from the point of view of power systems, consider the following DAE model of a power system:

$$\dot{x} = f(x, y, \lambda, p)$$
$$0 = g(x, y, \lambda, p) \tag{1}$$

where $x \in \Re^n$ is a vector of state variables, such as the generator frequencies; $y \in \Re^m$ is a vector of algebraic variables, such as the load voltage magnitudes and phase angles; $\lambda \in \Re^l$ is a set of uncontrollable parameters, such as active and reactive power load variations; and p is a set of controllable parameters such as the voltage regulator set points. When the parameter λ and /or p vary, the equilibrium points (x_o, y_o) change, and so do the eigenvalues of the corresponding system state matrix.

The equilibrium point where a complex conjugate pair of eigenvalues "crosses" the imaginary axis with respect to change in (λ, p), say $(x_o, y_o, \lambda_o, p_o)$, is known as a HB point.

At a HB point $(x_o, y_o, \lambda_o, p_o)$, the following conditions are satisfied [15]:

1. $\left[f(x_o, y_o, \lambda_o, p_o) g(x_o, y_o, \lambda_o, p_o) \right]^T = 0$.
2. The Jacobian or reduced system state matrix evaluated at the equilibrium point should have a simple pair of purely imaginary eigenvalues $\mu = \pm j\beta$.
3. The rate of change of the real part of the critical eigenvalues with respect to a varying system parameter, say λ, should not be zero.

If this is the case, a limit cycle appears at $(x_o, y_o, \lambda_o, p_o)$, with an initial period of $T_o = \dfrac{2\Pi}{\beta}$. These conditions imply that a HB corresponds to a system equilibrium state with a pair of purely imaginary eigenvalues with all other eigenvalues having non-zero real parts, and that the pair of bifurcating or critical eigenvalues cross the imaginary axis as the parameters (λ, p) change, yielding oscillations in the system.

Oscillatory problems in power systems are associated with a lack of damping on the critical modes. Thus considering a complex mode $-\alpha \pm j\beta$,

located in the open left half-plane, the damping ratio of the mode is then defined as:

$$\zeta = \frac{-\alpha}{\sqrt{\alpha^2 + \beta^2}} \qquad (2)$$

If the mode "travels" from left to right due to parameter changes, a change in the damping ratio of the critical mode occurs, with the damping ratio having a value between 1 and –1. A HB occurs at a point where damping of the mode becomes zero, i.e. at the point where the real part of the critical mode vanishes. For positive damping ratio, the critical mode is located in the open left half-plane and the corresponding small disturbance time domain response is oscillatory and stable. On the other hand, for a negative damping ratio, the critical mode is in the open right half-plane and the small disturbance time domain response is oscillatory and unstable. By adding controllers, such as PSS and/ or FACTS controllers it is possible to improve the damping on the critical mode hence delay or completely eliminate the HB. However, all these results are greatly influenced by the load models as demonstrated in this paper.

3. Models, Test System and Tools
3.1 Load Modeling

Load models are traditionally classified into two categories: Static and dynamic. In this paper, only the effect of static load models is considered; these types of loads are typically categorized as follows [12]:

Constant Impedance Load Model (Constant Z): The active and reactive powers are proportional to the square of the voltage magnitude.

Constant Current Load Model (Constant I): The active and reactive powers are directly proportional to the voltage magnitude.

Constant Power Load Model (Constant P): The active and reactive powers do not vary with changes in voltage magnitude.

Exponential Load Model: The powers are represented as an exponential expression as given in (3):

$$P_L = P_o \left(\frac{V}{V_o}\right)^\alpha ; Q_L = Q_o \left(\frac{V}{V_o}\right)^\beta \qquad (3)$$

Where P_o and Q_o stand for the real and reactive powers consumed at a reference voltage V_o, respectively. The exponents α and β depend on the type of load that is being represented, e.g. for constant power load model $\alpha=\beta=0$, for constant current load models $\alpha=\beta=1$ and for constant impedance load models $\alpha=\beta=2$.

Polynomial Load Models: The active and reactive powers are represented as a polynomial equation of voltage magnitude. It is usually referred to as ZIP model, as it is made up of three differential load models: Constant Impedance (Z), Constant Current (I), and Constant Power (P). The real and reactive power characteristics of the ZIP load models are given by (4):

$$P_L = P_o [a_p \left(\frac{V}{V_o}\right)^2 + b_p \left(\frac{V}{V_o}\right) + c_p]$$

$$Q_L = Q_o [a_Q \left(\frac{V}{V_o}\right)^2 + b_Q \left(\frac{V}{V_o}\right) + c_Q] \qquad (4)$$

Where $a_p + b_p + c_p = a_Q + b_Q + c_Q = 1$, and P_o and Q_o are the real and reactive power consumed at a reference voltage V_o.
In power flow, to obtain various equilibrium points along the PV curve, the loads are typically modeled as constant P loads with constant power factor, i.e.

$$P_L = P_{Lo}(1 + \lambda)$$
$$Q_L = Q_{Lo}(1 + \lambda) \qquad (5)$$

Where P_{Lo} and Q_{Lo} correspond to the base loading conditions and λ is the loading factor (L.F.), which typically represents a slow varying parameter used in bifurcation studies.

3.2 Test System

Figure 1 depicts the single line diagram of the IEEE 14 bus test system used in this paper. It consists of 14 buses, 20 branches, three transformers, and five synchronous machines

with IEEE Type 1 exciters, three of which are synchronous compensators used only for reactive power compensation. There are eleven loads in the system totaling 259 MW and 81.3 Mvar. The dynamic data for the generators and exciters were extracted from [16]. The location of the three different power system controllers considered for damping oscillations, i.e. PSS, SVC and TCSC are shown in Fig. 1.
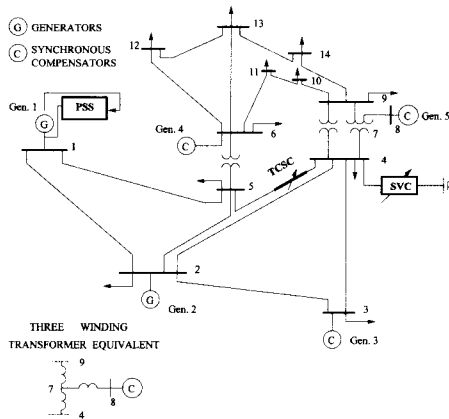

Fig. 1. IEEE 14 bus test system with various added controllers.

3.3 Tools

All the power flows and PV curve studies were carried out with the help of UWPFLOW [17], which is a program designed to study fold bifurcations, such as saddle-node and limit induced bifurcations, in power system using continuation and direct methods. Small-signal stability analyses were carried out using EPRI's Multi-Area Small Signal Stability program (MASS) [18].

4. Simulation Results and Discussion
4.1 Base Case

For the base system with no controllers and line outages, which is referred to as a the "base case", Fig. 2 depicts the PV curve, including the HB points for the test system with constant P ($\lambda=0.47$) and constant current I ($\lambda=0.6$) load models; there is no HB associated with the constant Z model.
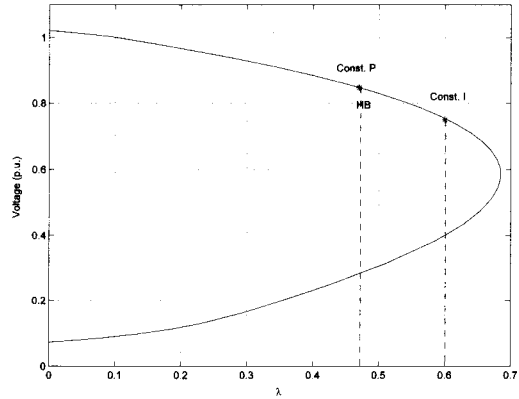

Fig. 2 PV curve at bus 14 for the test system.

Figure 3 and 4 depict the critical modes of the system for $\lambda=0$ and $\lambda=0.47$, respectively, for the load models. Observe that at low loading conditions, there is practically, no difference on the damping ratio for the critical modes among the different load models; however, as the loading increases, the difference becomes rather significant, with the constant P model reaching first a HB condition. The value of damping rations for the 4 most critical modes at $\lambda=0.47$ are shown in Table I for the three different load models considered here. These results are consistent with what can be found in the literature associated with power system stability, i.e. constants P load models stress the system the most, whereas constant Z models are the least demanding one.
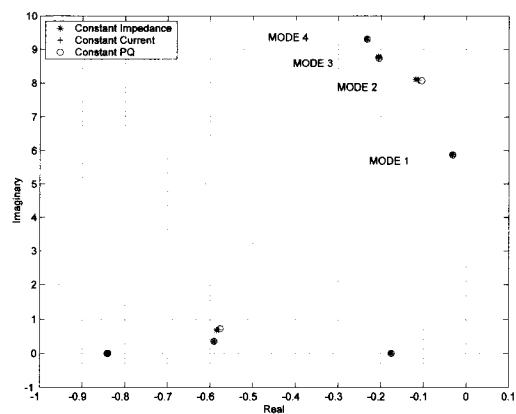

Fig. 3. Comparison of some critical modes for different static load models at $\lambda=0$.
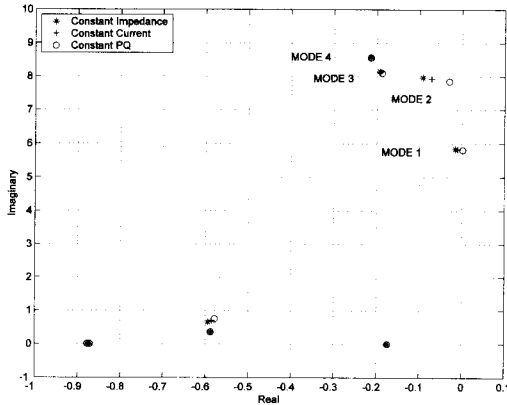
Fig. 4. Comparison of some critical modes for different static load models at λ=0.47.

Table I Damping Ratios of Critical Modes For Different Load Models at λ=0.47

Mode	Dom. State	Damping Ratio		
		Const. P	Const. I	Const. Z
1	δ_3, ω_3	-0.0003	0.0017	0.0026
2	δ_2, ω_2	0.0039	0.0097	0.0116
3	δ_5, ω_5	0.0232	0.0237	0.0238
4	δ_4, ω_4	0.0251	0.0250	0.0250

4.2 Line Outages

The influence of different static load models on HB is investigated here for the most severe line outages. Based on the results shown in Table II, one can observe that the different static load models behave in a similar way relative to each

other for the most severe system contingencies as for the base case, with the constant P load model yielding the lowest Dynamic Loading Margins (DLM), followed by the constant current I and Z models. The DLM is defined as the loading margin from λ=0 to the HB point, as depicted in the PV curves of Fig. 5 for constant P load model.

Table II DLM for Different Static Load Models and Contingencies

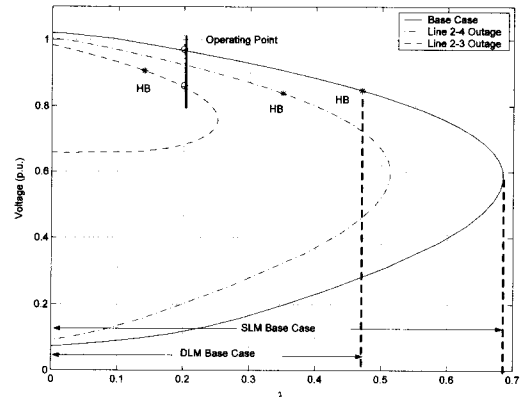|	Loading Margins (p.u.)		
	Const. P	Const. I	Const. Z
Base Case	0.47	0.60	0.68*
Line 2-4	0.35	0.46	0.51*
Line 2-3	0.14	0.17	0.25*

* Equal to SLM (see Fig. 5)

Fig.5. PV Curves at bus 14 for the test system with no controllers and constant P load model for the worst system contingencies.
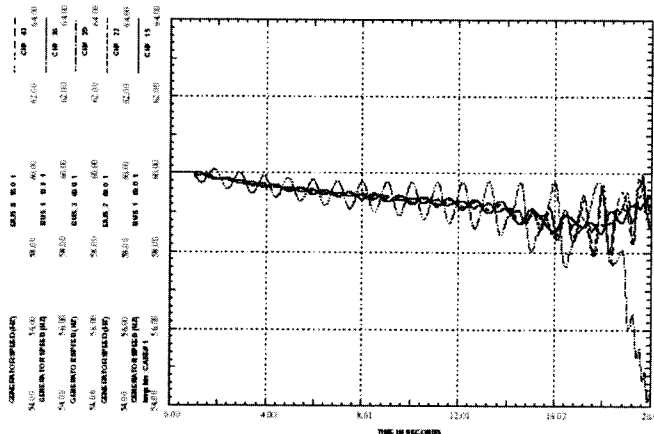

Fig. 6. Generator frequency oscillation due to HB triggered by line 2-3 outage in the test system with constant PQ loads at λ=0.2.

Figure 6 shows the oscillatory unstable condition due to the Hopf bifurcation triggered by line 2-3 outage, when the system operates at 0.2 p.u. As can be seen from Figs. 5 and 6, the post fault equilibrium point is an unstable point.

Once again, the damping ratios of the critical modes do not present any significant difference at low loading conditions, with the difference increasing as the loading level increases. As in the base case, the constant Z load model produces the highest damping followed by the constant I model and then the constant P model, which shows again that constant Z has the least onerous loads for the system.

4.3 Controller Impact

The effect of various controllers, namely, PSS, SVC and TCSC, on the HB and damping ratios of the critical modes for different load models is studied here.

A participation factor analysis indicates that the dominant state variables are associated with the HB mode are δ_3 and ω_3 of Gen. 3. However, PSS is installed in the next best location, which is Gen. 1, as Gen. 3 is a synchronous compensator where the PSS is not effective. The SVC and TCSC controllers are placed based on a maximum damping analysis of critical mode for the system with constant P load models. All controllers' locations are shown in Fig. 1.

PSS and SVC controllers eliminate the HB for all the different load models so that DLM in those cases is equal to SLM, as shown in Table III, for the base case and worst system contingencies. The TCSC controller eliminates the HB for the constant Z and constant I load models; however, it does not eliminate the HB for constant P load models, as shown in Table IV.

Table III DLM and SLM with PSS and SVC Controllers for All Load Models

Margin (p.u.)*	Base Case	Line 2-4 Outage	Line 2-3 Outage
PSS	0.68	0.51	0.25
SVC	0.82	0.65	0.38

* DLM=SLM

Table IV DLM and SLM with TCSC Controller for Constant P Model

Margin (p.u.)	Base Case	Line 2-4 Outage	Line 2-3 Outage
DLM	0.68	0.55	0.32
SLM	0.74	0.62	0.34

When the PSS or SVC controllers ᵃ introduced in the system, the damping ra⁺ ᵒn the critical mode is the lowest for the c⸗ ᵤnt impedance model and the highest for cor ₃tant P load models (see Tables V and VI). ⸗is is completely the opposite to what was observed for the cases without controllers, with PSS and SVC controllers adding more damping on the critical mode when the loads are represented as constant P loads for all system conditions, i.e. for low and high loading levels as well as for the worst system contingencies.

A similar result for a Brazilian power system has been reported in [19], where PSS with higher gain along with constant PQ loads yield higher damping ratio on the critical mode than the other two loads. Further investigations need to be carried out to find reasons behind this "contrary results" to a popular belief.

Table V Damping Ratio of Critical Modes at $\lambda=0.47$ with PSS Controller

Mode	Damping Ratio		
	Const. P	Const. I	Const. Z
1	0.0085	0.0071	0.0068
2	0.0158	0.0184	0.0197
3	0.0236	0.0237	0.0238
4	0.0253	0.0252	0.0252

Table VI Damping Ratio of Critical Modes at $\lambda=0.47$ with SVC Controller

Mode	Damping Ratio		
	Const. P	Const. I	Const. Z
1	0.0138	0.0122	0.0101
2	0.0116	0.0141	0.0156
3	0.0197	0.0263	0.0314
4	0.0246	0.0250	0.0253

Table VII shows the damping ratio of the 4 most critical modes at $\lambda=0.47$ for the system with

TCSC controller and different load models. In this case, the highest damping on the critical mode was obtained with constant Z load models.

Table VII Damping Ratio of Critical Modes at λ=0.47 with TCSC Controller

Mode	Damping Ratio		
	Const. P	Const. I	Const. Z
1	0.0021	0.0033	0.0038
2	0.0048	0.0095	0.0119
3	0.0235	0.0237	0.0237
4	0.0251	0.0251	0.0251

5. Conclusions

This paper studies in detail the effect of static load models on Hopf bifurcation in power systems. For a test system, the damping ratios of the most critical modes are analyzed for variety of system conditions and with different controllers. It is shown that constant P load models yield the lowest dynamic loading margin in most of the cases, followed by constant I and constant Z load models, in that order. This is consistent with observations made in previous studies available in the current power system stability literature. The damping ratio of the system critical modes, especially electromechanical modes, show significant difference as the load levels are increased for load models, stressing the importance of adequate load modeling in stability studies.

In general, constant P load models can be considered as the most onerous loads for the system from the stability point of view, suggesting that this type of load model may be the most appropriate for a variety of stability studies of systems where better load models are not available. However, it is shown here that when controllers are introduced in the system, other load models may yield more conservative results due to the presence of these controllers, highlighting the need to carry out stability studies considering not only a variety of system conditions but multiple load models as well.

6. References

[1] N. Mithulananthan, C. A. Canizares, J. Reeve and Graham J. Rogers, Comparison of PSSs, SVC and STATCOM Controllers for Power System Oscillations, *IEEE Trans. Power System*, Vol. 18, No. 2, pp. 786-792, May 2003.

[2] E. H Abed and P. P. Varaiya, Nonlinear Oscillation in Power Systems, *International Journal of Electric Power and Energy System*, Vol. 6, pp. 37-43, 1984.

[3] C. D. Vournas, M. A. Pai and P. W. Sauer, The Effect of Automatic Voltage Regulation on the Bifurcation Evolution in Power Systems, *IEEE Trans. Power System*, Vol. 11, No. 4, pp. 37-43, 1996.

[4] N. Mithulanathan and S. C. Srivastava, Investigation of a Voltage Collapse Incident in Sri Lankan Power System Network, *Proc. of EMPD 98*, pp. 47-52, March 1998.

[5] C. Alsberg, WSCC issues Preliminary Report of August Power Outage: PRESS RELEASE, technical report, WSCC, September 1996.

[6] N. Mithulananthan, C. A. Cañizares, and J. Reeve, Hopf Bifurcation Control in Power Systems Using Power System Stabilizers and Static Var Compensators, *Proc. NAPS-1999*, San Luis Obispo, CA, pp. 155-162, October 1999.

[7] A. I. Zecevic and D. M. Miljkovic, The Effect of Generation Redispatch on Hopf Bifurcations in Electric Power System, *IEEE Trans. on Circuit and Systems I*, Vol. 49, No. 8, pp. 1180-1186, August 2002.

[8] A. A. P. Lerm, Control of Hopf Bifurcation in Multi-area Power System Via a Secondary Voltage Regulation Scheme, *Proc. of IEEE/PES Summer Meeting*, pp. 1615-1620, July 2002.

[9] C. A. Cañizares, On Bifurcations, Voltage Collapse and Load Modeling, *IEEE Trans. Power System*, Vol. 10, No. 1, pp. 512-522, February 1995.

[10] CIGRE Study Committee 38, Load Modeling and Dynamics, technical report, 1990.

[11] IEEE Task Force, Load Representation for Dynamic Performance Analysis, *IEEE PWRS*, Vol. 8, No.2, pp. 472-482, 1993.

[12] P. Kundur, *Power System Stability and Control*, McGraw Hill, New York, 1994.

[13] S. Z. Zhu, J. H. Zheng, S. D. Shen, and G. M. Luo, Effect of Load Modeling on Voltage Stability, *IEEE/PES Summer Meeting*, Vol. 1, pp. 395-400, 2000.

[14] J. Li and V. Venkatasubramanian, Study of Hopf Bifurcation in a Simple Power System Model, *Proc. of 39ᵗʰ Conference on Decision and Control*, pp. 3075-3079, December 2000.

[15] R. Seydel, *Practical Bifurcation and Stability Analysis: From Equilibrium to Chaos*, Second Edition, Springer-Verlag, New York, 1994.

[16] P. M. Anderson and A. A. Found, *Power System Control and Stability*, IEEE Press, 1994.

[17] C. A. Cañizares, et. al, UWPFLOW: Continuation and Direct Methods to Locate Fold Bifurcations in AC/DC/FACTS Power Systems, University of Waterloo, available at http://www.power.uwaterloo.ca, August 1998.

[18] Small Signal Stability Analysis Program: Version 31. EPRI, May 1994.

[19] N. Martins and L. T.G. Lima, Eigenvalue and Frequency Domain Analysis of Small-Signal Electromechanical Stability Problems, *Proc. IEEE* Symposium on Application of Eigenanalysis and Frequency Domain Method for System Dynamic Performance, pp. 17-33, 1989.